Evaluation Perceptual Color Edge Detection Algorithms

Aurora Sáez, Carmen Serrano, Begoña ***Acha, Signal Processing and Communications Department, University of Seville, Spain***

Abstract

Although several colour edge detectors have been proposed, all of them utilized colour Euclidean distances in the colour space to measure colour differences. In this paper a set of colour edge detection algorithms based on colour visual perception is proposed. These algorithms are a combination of vector edge detector, in uniform colour spaces and using perceptual colour difference equations. A comparative study has been performed. To evaluate the detectors performance a set of synthetics images is generated and various measures are used. It can be concluded that detectors based on CIEDE2000 colour difference equation are better regarding the correlation with colour visual perception.

Introduction

Edge detection is one of the fundamental operations in computer vision. Edges correspond to abrupt discontinuities in physical quantities such as gray-level, color, texture or motion. In order to analyse an image, the human visual system detects changes in it, that is, discontinuities. Several colour edge detector preserving Nowadays, the majority of the image processing tasks are developed for colour images. The advantage of color edge detection schemes over grayscale approaches is easily demonstrated by considering the fact that those edges that exist at the boundary between regions of different colors cannot be detected in grayscale images if there is no change in intensity [1]. The color edge detectors can be classified into two groups: those techniques extended from grayscale edge detectors which apply the detection method in each color plane and combining the results, and those techniques that take into account the vector nature of the color images. Several colour edge detector preserving this vector nature have been proposed [2] but all of them utilized Euclidean distances in the colour space to measure colour differences.

In order to detect edges extending the concept of derivative operator to three-color-component pixels, different algorithms have been developed in the literature. One of simplest approximations consists in generalizing the operators based on the first derivative, e.g. Sobel, commonly applied in the grayscale images into the multidimensional case. Wesolkowski compared several edge detectors in multiple colour spaces, and he drawed the conclusion that the performance of Sobel operator is superior to others [3]. Therefore Sobel operator is used in this paper. Other vector approach was proposed by DiZenzo [4] who extended the gradient based edge detection technique to colour images combining the three colour components using a tensor structure. The algorithm computed the magnitude and the maximal direction of the gradient. These approaches were based on the RGB colour space and the Euclidean distance. To achieve results that are correlated with perceptual colour differences, RGB space is avoided because it is not a perceptually uniform colour space, and we make use of a perceptual uniform colour space (CIE L*a*b*) and CIE94 and CIEDE2000 colour difference equations.

In this paper three detectors based on perceptual vector edge detectors are proposed. A comparative study between these detectors and the traditional Canny operator is carried out. To evaluate the performance of the detectors a database formed by 48 images has been generated, and both quantitative and qualitative measures are used to test which is the correlation between the detector output and visually perceived colour differences.

Methodology

General scheme

The proposed method performs the following steps:

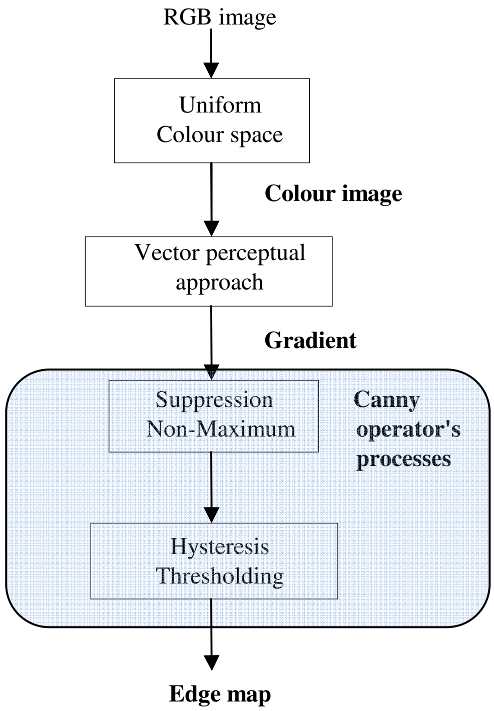

Figure 1. General description of the algorithm

Each step is explained in the following subsections.

Perceptual Uniform Colour Space

In 1976, CIE standardized $L^*a^*b^*$ space, also called CIELAB, as perceptually uniform [5]. *Perceptually uniform* means that changes in colours measure with Euclidean distances correspond to perceptual colour differences. The three coordinates of CIELAB represent the lightness of the colour (L^*), its position between red/magenta and green (a^*) and its position between yellow and blue (b^*). It can also be expressed in terms of cylindrical coordinates with the perceived lightness L^*, the chroma C_{ab}^* and the hue h_{ab}^*, defined in equation (1) and (2) respectively.

$$C^*_{ab} = \sqrt{(a^*)^2 + (b^*)^2} \quad (1)$$

$$h_{ab} = \arctan\left(\frac{b^*}{a^*}\right) \quad (2)$$

Colour differences are measured in the CIELAB space with the Euclidean distance between the coordinates for the two stimuli. This is expressed in terms of CIELAB as ΔE^*_{ab}, which can be calculated using equation (3).

$$\Delta E^* = \sqrt{(\Delta L^*)^2 + (\Delta a^*)^2 + (\Delta b^*)^2} \quad (3)$$

where $\Delta L = L_1 - L_2$ (Δa and Δb are defined in the same manner for coordinates a and b). However, it has been demonstrated that Euclidean distance ΔE^* is not an accurate measure of perceived colour difference between two stimuli. To correct the problem a new difference formula was recommended in 1994 by CIE [6].

$$\Delta E^*_{94} = \sqrt{\left(\frac{\Delta L^*}{k_L S_L}\right)^2 + \left(\frac{\Delta C^*_{ab}}{k_C S_C}\right)^2 + \left(\frac{\Delta H^*_{ab}}{k_H S_H}\right)^2} \quad (4)$$

$$S_L = 1 \quad (5)$$

$$S_C = 1 + 0.045 C^*_{ab} \quad (6)$$

$$S_H = 1 + 0.015 C^*_{ab} \quad (7)$$

The factors k_L, k_C and k_H, are included to match the perception of the background conditions. Nevertheless, effects of non-uniformity in this space for small colour differences in different ranges and different directions have been tested. Other new formulation, CIEDE2000, tries to correct them.

$$\Delta E_{00} = \sqrt{\left(\frac{\Delta L'}{k_L S_L}\right)^2 + \left(\frac{\Delta C'}{k_C S_C}\right)^2 + \left(\frac{\Delta H'}{k_H S_H}\right)^2 + R_T\left(\frac{\Delta C'}{k_C S_C}\right)\left(\frac{\Delta H'}{k_H S_H}\right)} \quad (8)$$

where ΔC and $\Delta H'$ are defined in ref. [7].

Vector perceptual approaches

In vector methods the vector nature of colour is preserved throughout the computation. Colour images can be viewed as a two-dimensional three channel vector field which can be characterized by a discrete integer function f(x,y). The value of this function at each point is defined by a three dimensional vector in a given colour space. Therefore, a pixel is defined as shows equation (9).

$$\mathbf{f}(x,y) = \begin{bmatrix} C_1(x,y) \\ C_2(x,y) \\ C_3(x,y) \end{bmatrix} \quad (9)$$

where $C_i(x,y)$ represents the value of the pixel in the i-th colour plane (i=1,2,3), and (x,y) refers to the spatial dimensions in the 2-D plane.

Color Sobel Detector

Sobel masks are applied to $L^*a^*b^*$ image. They can be applied by constructing the vectors: $V_1^+=a_3+2a_6+a_9$, $V_1^-=a_1+2a_4+a_7$, $H_1^+=a_7+2a_8+a_9$, $H_1^-=a_1+2a_2+a_2$, according to the notation used in Figure 2. In equation (10) and (11) the gradients along x and y direction respectively, are shown.

$$G_x = \Delta E(\boldsymbol{V}_1^+, \boldsymbol{V}_1^-) \quad (10)$$

$$G_y = \Delta E(\boldsymbol{H}_1^+, \boldsymbol{H}_1^-) \quad (11)$$

where ΔE denotes the colour difference between two vectors. This paper proposes that ΔE is determined by CIE94 and CIEDE2000.

a_1	a_2	a_3
a_4	a_5	a_6
a_7	a_8	a_9

Figure 2. *3×3 colour Sobel detector mask*

The gradient magnitude and the direction are computed as shown in equations (12) and (13).

$$G = \sqrt{{G_x}^2 + {G_y}^2} \quad (12)$$

$$\theta = \arctan\left(\frac{G_y}{G_x}\right) \quad (13)$$

Tensor gradient

The computation of this tensor gradient was introduced by DiZenzo. Drewniok in 1994 [8] provided a more general approach for the multi-dimensional edge detection. The algorithm is an eigenvector-based approach which guarantees good localization of the edge structures in some parts of the image where data are correlated, while at the same time it integrates uncorrelated structures from different spectral channels.

In this approach the cylindrical coordinates of $L^*a^*b^*$ space, i.e. the lightness L^*, the chroma C_{ab}^* and the hue h_{ab}^* are used. The choice of $L^*C_{ab}^*h_{ab}$ space is motivated by the CIE94 colour difference, which is based on weighted Euclidean distance.

Therefore, let $\mathbf{f}(x,y)=[C_1(x,y),C_2(x,y),C_3(x,y)]$, where $C_1(x,y)=L^*(x,y)$, $C_2(x,y)=C^*_{ab}(x,y)$ and $C_3(x,y)=h_{ab}(x,y)$. The direction $\mathbf{n}$ is defined by the angle φ in equation (14).

$$\mathbf{n} = \begin{bmatrix} \cos\varphi \\ \mathrm{sen}\ \varphi \end{bmatrix} \quad (14)$$

The directional derivative of $\mathbf{f}(x,y)$ is:

$$\frac{\partial \mathbf{f}(x,y)}{\partial n} = \begin{bmatrix} \frac{\partial C_1(x,y)}{\partial n} \\ \frac{\partial C_2(x,y)}{\partial n} \\ \frac{\partial C_3(x,y)}{\partial n} \end{bmatrix} = \begin{bmatrix} \nabla C_1(x,y)\cdot\mathbf{n} \\ \nabla C_2(x,y)\cdot\mathbf{n} \\ \nabla C_3(x,y)\cdot\mathbf{n} \end{bmatrix} = \begin{bmatrix} C_{x,1} & C_{y,1} \\ C_{x,2} & C_{y,2} \\ C_{x,3} & C_{y,3} \end{bmatrix} \cdot \mathbf{n} = \mathbf{J}\cdot\mathbf{n} \quad (15)$$

where $C_{x,i}$ and $C_{y,i}$ are the derivatives of the i-th component in the x and y direction respectively and $\mathbf{J}$ is the Jacobian matrix. The Euclidean norm:

$$\left\|\mathbf{J}^{\mathbf{T}}\cdot\mathbf{n}\right\| = (\mathbf{J}\cdot\mathbf{n})^{\mathbf{T}}(\mathbf{J}\cdot\mathbf{n}) = \mathbf{n}(\mathbf{J}^{\mathbf{T}}\cdot\mathbf{J})\mathbf{n} \quad (16)$$

where:

$$\left(\mathbf{J}^{\mathbf{T}}\mathbf{J}\right)=\begin{bmatrix} \sum_{i=1}^{3}(C_{x,i})^2 & \sum_{i=1}^{3}C_{x,i}\cdot C_{y,i} \\ \sum_{i=1}^{3}C_{x,i}\cdot C_{y,i} & \sum_{i=1}^{3}(C_{y,i})^2 \end{bmatrix}=\begin{bmatrix} a_{11} & a_{12} \\ a_{21} & a_{22} \end{bmatrix} \quad (14)$$

represents the norm of the color directional derivative in direction **n.** The magnitude of the strongest change of **f** coincides with the largest eigenvalue, and the direction of the strongest change is the direction of the corresponding eigenvector of the matrix $\mathbf{J}^{\mathbf{T}}\mathbf{J}$ (equation (18) and (19)).

$$\lambda_{\max}=\frac{1}{2}\left(\left(a_{11}+a_{22}\right)+\sqrt{\left(a_{11}-a_{22}\right)^2+4a_{12}^2}\right) \quad (18)$$

$$\varphi_{\max}=\arctan\left(\frac{\lambda_{\max}-a_{11}}{a_{12}}\right) \quad (19)$$

Sobel operators can be used to compute the partial derivatives of each color plane in the x and y directions, i.e., $C_{x,i}$ and $C_{y,i}$.

In summary three detectors from three vector edge detectors are obtained:

- Vectorial Sobel in $L^*a^*b^*$, that computes distances using CIE94
- Vectorial Sobel in $L^*a^*b^*$, that computes distances using CIEDE2000
- Tensor gradient in $L^*C_{ab}^*h_{ab}^*$

Non-maxima-suppression process and hysteresis thresholding

The last two steps are precisely the last two steps of Canny operator, which aim accuracy in the edge detection.

- Non-maxima-suppression process:

To guarantee the precision of edge location, the gradient amplitude of the image should be refined. Edge magnitude may contain wide ridges around the local maxima. Non maxima suppression removes the non maxima pixels preserving the connectivity of the contours. If the gradient magnitude value of a pixel (x,y) is less than at least one of its neighbor along gradient direction, this pixel is marked as background (suppression), otherwise the pixel is marked as an edge. This process is explained in Figure 3. If M(P) (gradient magnitude of pixel P) is less than M(A) or than M(B) (gradient magnitude of the two neighbour pixels along gradient direction), the pixel P is discarded as a contour. The gradient magnitude of A and B are linearly interpolated between the closest points in the neighborhood. The value at A is interpolated between the values at P7 and P8 and the value at B between those at P3 and P4.

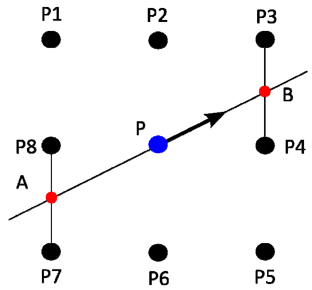

Figure3. Non-maxima suppression method. Checking whether P pixel is a local maximum of the magnitude of the gradient in the direction of the gradient is done by interpolating the gradient magnitude at A and B.

- Hysteresis thresholding:

Hysteresis uses 2 thresholds, a high one (T_{high}) and a low one (T_{low}).

If $M(P) > T_{high}$, P is considered edge (strong edge)
If $M(P) < T_{low}$, P is not considered edge
If $T_{low} \leq M(P) \leq T_{high}$, P is considered edge if only if it is connected to a strong edge.

Therefore, edge pixels stronger than the high threshold are marked as strong; edge pixels weaker than the low threshold are suppressed and edge pixels between the two thresholds are marked as weak. Strong edges are interpreted as “certain edges”, and can immediately be included in the final edge image. Weak edges are included if and only if they are connected to strong edges.

Results

A comparative study between the three proposed perceptual detectors and the traditional Canny operator is carried out to test which one is more correlated with colour visual perception.

To evaluate the performance of the detectors a database formed by 48 images has been generated. Then, evaluation procedures defined by Plataniotis [9], have been carried out. Both quantitative and qualitative measures are used. The quantitative performance measures are based on edge deviation from true edges. For this experiment a predefined edge map (ground truth) is required. As our images are synthetic the ground truth is known. Since numerical measures are not sufficient to model the complexity of human visual systems, qualitative evaluation is needed. This measure allows us to test which is the correlation between the detector output and visually perceived colour differences.

Images database

A set of colour discrimination data has been created. The experiment was carried out to evaluate edge detector performance regarding to two approaches: how much the detected edge deviates from the true edges (since images are synthetic we know the ground truth), and how much the edge detection is correlated with the visually perceived colour differences (since images show pair of colours with different CIELAB colour values between them).

In 1978, CIE published guidelines [10] to co-ordinate researchers who study colour differences. Five colour centers were recommended for study. Our images are based on these centers, which are shown in Table I.

Table I. The CIELAB values of colour centers

Colour	L^*	a^*	b^*	C^*	h
Gray	63.5	-0.6	0.8	0.9	126.4
Red	46.2	37.8	23.8	44.7	32.2
Yellow	87.9	-6.6	46.1	46.5	98.2
Green	58.6	-33.7	0.8	33.7	178.7
Blue	37.3	4.7	-32	32.3	278.3

Colour pairs with different CIELAB units (Euclidean distance in $L^*a^*b^*$) between them were generated. The set is formed by 48 images. Four squares are represented in each image. Two of them correspond to two colour centers shown in Table I. The others two correspond to colours with an amount of CIELAB units from the two centers. This amount is 0.5, 2, 4, 6, 8 or 10 CIELAB units. In figure 4 an example of two images from the dataset is shown.

a) b)

Figure4. Example of images from the dataset. a) Sample pairs with 0.5 CIELAB units. b) Sample pairs with 8 CIELAB units

In figure 4 a) there is a small square inside the green zone with 0.5 CIELAB units regard to green center shown in Table I. The same occurs inside the yellow zone, however human visual system cannot perceived this difference. Nevertheless in figure 4 b) there is 8 CIELAB units between samples and they are already perceived by the human visual system.

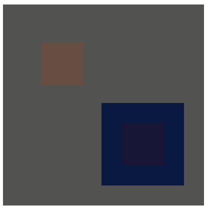

Figure5. Example of images with same CIELAB units between two pairs but different visual perception

It is also interesting to note that for two sample pairs with the same CIELAB units between them, visual assessment may be not equal. An example of this is illustrated in figure 5, where the difference in terms of CIELAB units between gray samples is the same than between the blue samples, but they are not representing the same perceptual difference. We perceive more difference between the gray pair than the blue pair. However, this perceptual difference is represented by CIE94 and CIEDE2000 equations. Results in CIELAB, CIE94 and CIDE2000 units are shown in Table II. Values in CIE94 units and CIEDE2000 units are lower for the blue pair than the gray pair as human eye perceives them.

Table II. Differences between gray pair and blue pair of Figure 5.

	CIELAB	CIE94	CIEDE2000
Gray	10	9.613	10.259
Blue	10	4.17	5.6

More examples of images from dataset are shown in figure 6.

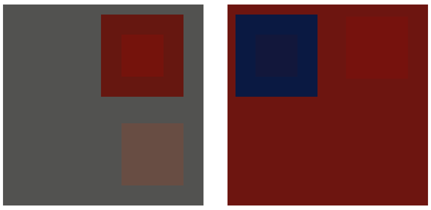

a) b)

Figure6. Example of images from the dataset. a) Sample pairs with 10 CIELAB units. b) Sample pairs with 6 CIELAB units

Evaluation of results

Two measures to evaluate the resulting edge maps are carried out.

Subjective test

Subjective evaluation is very important in image processing [9]. Moreover, as the aim of our work is to perform visually perceived colour differences study, this step becomes essential.

Six observers were asked to say the number of different colours that they could distinguish in each image. The final decision for each image is the number of colours most voted by the observers. If the detector output coincides with this result its hit ratio increases. Each detector hit ratio is summarized in Table III.

Table III. Subjective test results.

	Traditional Canny	Tensor gradient	Sobel using CIE94	Sobel using CIE00
Hit Ratio	62.5%	70.83%	72.92%	$\boxed{83.3\%}$

As is shown in Table III, the detector based on Sobel using CIEDE2000 has a performance more correlated with what human eye perceive.

Quantitative measure

The resulting edge maps from the developed detectors are compared with the results of the traditional Canny method operated on grayscale. Edge merit E suggested by Pratt [11] is used. It is defined in equation (20).

$$E = \frac{\sum_{i=1}^{I_D} \left(\frac{1}{1+\alpha d(i)^2} \right)}{\max(I_D, I_I)} \tag{20}$$

where I_D is the amount of pixels that returns the detector, I_I is the amount of real pixels belonging to an edge, *d*(*i*) is the distance between the *i*-th pixel of the detector edge map and the pixel from the nearest real edge of the image, α is a scaling constant with usual value 1/9. When *E* value is 1, computed edge matches real edge.

All images have the same ground truth, but for some images the human visual system cannot completely perceive it. An example of this is illustrated in Figure 4 a), the image is formed by several objects but we can only perceived two of them. This is the reason why the subjective test is carried out. Results for Figure 4 b) are shown in Figure 7.

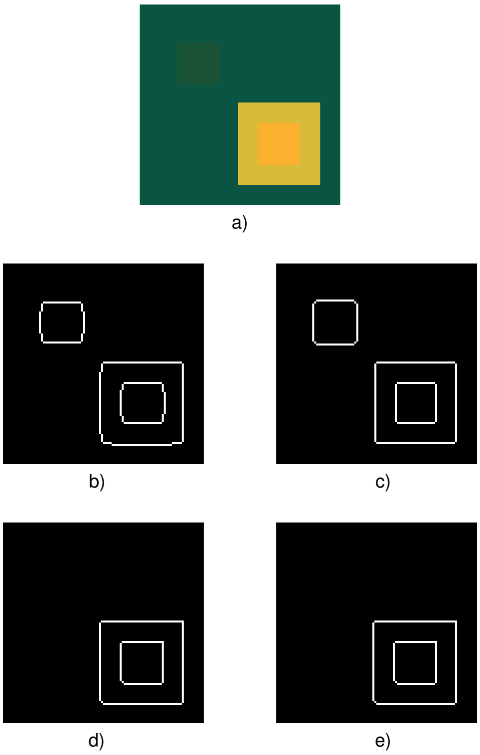

Figure 7. a) Test image. b) Output of Canny edge detector. c) Output of detector based in tensor gradient in $L^*C^*_{ab}h_{ab}$ space. d) Output of detector based in Sobel computed with CIE94. e) Output of detector based in Sobel computed with CIEDE2000.

Therefore, after the subjective test we can interpret that for each image there is a second ground truth, i.e. the ground truth that observers perceive. In Table IV the *E* mean value of each detector is shown. For each detector there are two E values, one corresponding to the global ground truth and the other to the resulting ground truth of the observers.

Table IV. Objective evaluation results.

	Traditional Canny		Tensor gradient	
	Mean	**Var.**	**Mean**	**Var.**
Global ground truth	0.6880	0.0398	0.6684	0.0393
Observer ground truth	0.8354	0.0191	0.8690	0.0199

Table IV. Objective evaluation results.

	Sobel using CIE94		Sobel using CIE00	
	Mean	**Var.**	**Mean**	**Var.**
Global ground truth	0.6308	0.0356	0.6330	0.0361
Observer ground truth	0.8825	0.0150	0.8932	0.0149

The best result is marked in red and corresponds to the detector based on Sobel using CIEDE2000 difference equation.

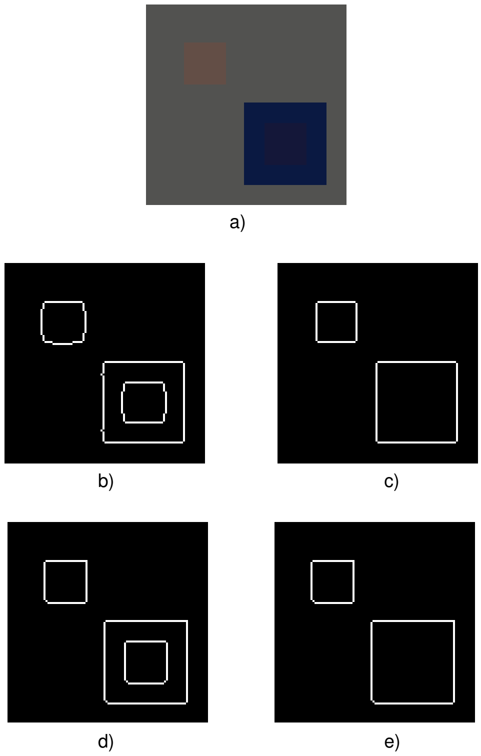

Figure 8. a) Test image. b) Output of Canny edge detector. c) Output of detector based in tensor gradient in $L^*C^*_{ab}h_{ab}$ space. d) Output of detector based in Sobel computed with CIE94. e) Output of detector based in Sobel computed with CIEDE2000.

In Figure 8 c), d) and e) is evident the improvement in accuracy. The results of c) and e) are more correlated with visual perception than the result in Figure b) and d), because in the test image it can be perceived colour difference between gray samples, however in blue samples is almost imperceptible.

Conclusions

In this paper an algorithm for colour edge detection is proposed. The algorithm is based on perceptual gradients. These gradients are computed by vector detectors in uniform colour spaces and using perceptual colour difference equations. A comparative study between the proposed perceptual detectors and the traditional Canny operator is carried out to test which one is more correlated with colour visual perception. To achieve this, a database formed by 48 images has been generated and evaluation procedures have been carried out. Experimental results show that the performance of the detector based on CIEDE2000 formula is more correlated with perceived colour difference. And the accuracy results demonstrate a superiority of the proposed operators over traditional Canny.

References

[1] Evans, A.N., Liu X.U. "A morphological gradient approach". *IEEE Transaction on Image Processing, Vol.*15 No.6 pp.1454-1563, 2006.

[2] Plataniotis K.N., Venetsanopoulos A.N., "Color Image Proseccing and Applications" *Color Image Processing and Applications*, Springer-Verlag, Berlin, 2000.

[3] Wesolkowski, S., Jernigan, M.E., Dony, R.D., “Comparison of color image edge detectors in multiple color space”. *ICIP*, pp. 796 – 799, 2009.
[4] DiZenzo, S., “A note on the gradient of a multi-image,” *Comput. Vis. Graph. Image Process.*, vol. 33, pp. 116–125, 1986.
[5] McLaren, K., " The development of the CIE 1976 (L*a*b*) uniform colour-space and colour-difference formula", *Journal of the Society of Dyers and Colourists 92*, pp. 338-341, 1976.
[6] CIE Publication 116. Industrial color-difference evaluation. Vienna, Austria, 1995.
[7] CIE, “Improvement to industrial colour-difference evaluation” CIE Publication No.142-2001, Cnetral Bureau of the CIE, Vienna, 2001.
[8] Drewniok, C., "Multi-sepctral edge detection. Some experiments on data from Landsat- TM", *International Journal of Remote Sensing* Vol. 15, No.18, pp. 3743-3765, 1994.
[9] Zhu, S.-Y., Plataniotis, K.N., Venetsanopoulos, A.N. "Comprehensive analysis of edge detection in color image processing ". Optical Engineering Vol. 38 N0.4, pp. 612-625, 1999.
[10] Robertson, A.R., " CIE guidelines for coordinated research on colour-difference evaluation" , *Color Res. Appl.* Vol. 3, No.3, pp. 149-151, 1987
[11] W.K. Pratt, Digital Image Processing, Wiley, New York,1978.

Author Biography

Aurora Sáez Manzano obtained her Telecommunication Engineering degree from University of Seville (Spain) in 2008. She also received her Technical Industrial Engineering degree (majoring in electronic engineering) from Universidad Cordoba (Spain) in 2003. She currently works in the Signal Processing and Communications Department of the University of Seville. Her research activities are focused on color image processing